Smart Structures and Systems, *Vol. 14, No. 4 (2014) 643-658*
DOI: http://dx.doi.org/10.12989/sss.2014.14.4.643

Servo control of an under actuated system using antagonistic shape memory alloy

S. Sunjai Nakshatharan[a], K. Dhanalakshmi * and D. Josephine Selvarani Ruth[b]

Department of Instrumentation and Control Engineering, National Institute of Technology, Tiruchirappalli, India

(Received June 23, 2013, Revised October 27, 2013, Accepted October 29, 2013)

Abstract. This paper presents the design, modelling and, simulation and experimental results of a shape memory alloy (SMA) actuator based critical motion control application. Dynamic performance of SMA and its ability in replacing servo motor is studied for which the famous open loop unstable balancing ball and beam system direct driven by antagonistic SMA is designed and developed. Simulation uses the mathematical model of ball and beam structure derived from the first principles and model estimated for the SMA actuator by system identification. A PID based cascade control system consisting of two loops is designed and control of ball trajectory for various target positions with settling time as control parameter is verified experimentally. The results demonstrate the performance of SMA for a complicated i.e., under actuated, highly nonlinear unstable system, and thereby it's dynamic behaviour. Control strategies bring out the effectiveness of the actuator and its possible application to much more complex applications such as in aerospace control and robotics.

Keywords: shape memory alloy; ball and beam system; dynamic behaviour; PID control; system identification

1. Introduction

Shape memory alloy (SMA) are active metallic "smart" materials used as actuators in high technology smart systems. The term SMA is becoming more and more synonymous with servo control application and many literatures discuss about position control application in robotics and automation using shape memory alloy (Moallem and Tabrizi 2008, Williams *et al.* 2010, Ruth *et al.* 2012, Mohammad *et al.* 2006, Singh and Anathasuresh 2013, Sars *et al.* 2010). There is wide proposal in applying SMA for some of the critical applications like position control of aerospace structure, flap control, morphing aero structure, micro air vehicle and unmanned aerial vehicle control (Ahn 2012, Tharayil and Alleyne 2004, Georges *et al.* 2009, Song *et al.* 2011) and for structural vibration suppression (Youssef and Elfeki 2012). But study of performance of SMA for such applications in real flight condition is still in the research phase. Mostly SMA is tested under very low frequency of operation. Though use of SMA is proposed for flight control application, no

∗Corresponding author, Associate Professor, E-mail: dhanlak@nitt.edu
[a] M.S. scholar, E-mail:sunjainakshatharan@gmail.com
[b] Ph.D. scholar, E-mail: djsruth@gmail.com

http://www.techno-press.org/?journal=sss&subpage=8 ISSN: 1738-1584 (Print), 1738-1991 (Online)

literature addresses the problem of stability in aero structure which requires actuators that deliver extreme performance. Hence any actuator that guides the aerospace system should be able to deliver the required stable performance. Testing SMA for such a system will be highly expensive and experimenting its behaviour by taking to actual flight is almost impossible. To analyse such behavioural system it is necessary to carry out experiments that may try to simulate closely the possible condition and also be simple to realize. One such system that has similar dynamics to that of an aircraft, simple and inexpensive to be tested in a laboratory is the famous classical control ball and beam system. The apparatus model the problems that control engineers have to address, in order to stabilise and optimise the system performance. Other examples of naturally unstable system represented by the ball and beam apparatus are the missile (rocket) or space shuttle launch and self-balancing robots. Further the ball and beam is an under actuated system, where ball position is controlled by the angular movement of the beam. The control of under-actuated systems is challengeable and attracts a worthy discussion. This paper introduces a new SMA based actuator for the highly dynamic ball and beam system and its performance is studied for motion control.

The organisation of this paper is as follows. Section 2 gives the system description of SMA driven ball and beam system and antagonistic actuator design. In Section 3, mathematical modelling of ball and beam and, model estimation of actuator assembly are presented. Section 4 describes the controller design, control strategy and experimental results followed by conclusion in section 5.

2. System Description

The ball and beam apparatus present problems of control to study the dynamics, modelling and realizing various controller designs. The system comprises of the ball and beam hinged at the centre and an actuation means to make partial rotation about a limited angle.

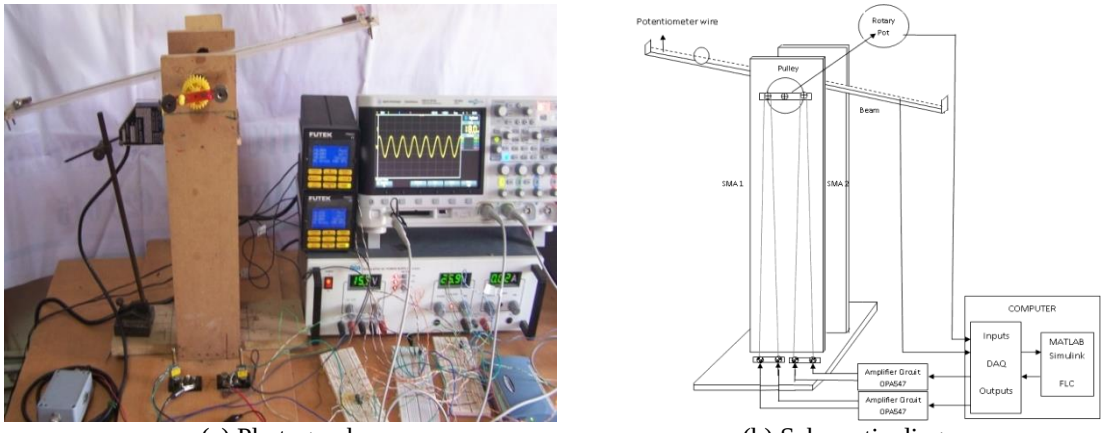

(a) Photograph (b) Schematic diagram

Fig. 1 Experimental setup

Table 1 Ball and beam specifications

Ball and beam specifications	Value
Length of the beam(cm)	60
Width of the beam(cm)	4
Thickness of the beam(cm)	0.20
Mass of the beam (kg)	0.153
Mass of the ball(kg)	0.023
Radius of the ball(cm)	0.8

2.1 Ball and beam system

The ball and beam apparatus consists of a steel ball rolling on a beam. Beam is normally horizontal, but it can be rotated through an angle of ± 20° by an actuator usually the electrical motor where in this case beam is rotated by antagonistic SMA. The beam angle θ is sensed by a laser displacement sensor mounted to the rear side of the beam shaft. Ball position is sensed by a linear potentiometer consisting of two parallel nichromewires. These wires are stretched along the top of the beam such that the steel ball may roll along the length of the beam, supported by the wires. One of the wires is connected to a voltage source. When the ball rests between the wires it allows a fraction of the source voltage to be measured at the other wire using potentiometer techniques. The output signal is proportional to the ball position *x* on the beam. A PC with Matlab/Simulink with Real Time Toolbox can be used to model and control. The sensors and actuators are interfaced through a data acquisition system. The schematic setup and photograph is shown in below Fig. 1.

2.2 SMA actuator design

The essence of this work is in the usage of SMA for actuation such that the study evaluates the ability of light weight, high force to mass ratio and compact actuator for the highly dynamic system. Antagonistic SMA configures the actuator assembly; its design is as follows:

The work generation potential of antagonistic shape memory actuators is determined by specific SMA element characteristics and their assembly conditions (Dhanalakshmi *et al.* 2011). In this work two SMA wires are connected in antagonism to apply forces alternatively to a circular disc with pulleys, in opposite direction in order to track any input signal as shown in Fig.1. Based on the literature (Moallem and Tabrizi 2008, Liang and Rogers 1990, Ruth *et al.* 2013), each SMA follows the stress-strain relationships given by Eqs. (1) and (2)

$$\dot{\sigma_1} = \frac{\Omega\varepsilon_{1T}(\tau_{1,}\sigma_1)+\theta_t}{1-\Omega\varepsilon_1(\tau_{1,}\sigma_1)}\alpha_1 i_1^2 + \frac{D}{1-\Omega\varepsilon_1(\tau_{1,}\sigma_1)}\dot{\varepsilon_1} - \frac{\Omega\varepsilon_1(\tau_{1,}\sigma_1)+\theta_t}{1-\Omega\varepsilon_1(\tau_{1,}\sigma_1)}\beta_1(T_1 - T_a) \quad (1)$$

$$\dot{\sigma_2} = \frac{\Omega\varepsilon_{2T}(\tau_{2,}\sigma_2)+\theta_t}{1-\Omega\varepsilon_2(\tau_{2,}\sigma_2)}\alpha_2 i_2^2 + \frac{D}{1-\Omega\varepsilon_2(\tau_{2,}\sigma_2)}\dot{\varepsilon_2} - \frac{\Omega\varepsilon_2(\tau_{2,}\sigma_2)+\theta_t}{1-\Omega\varepsilon_2(\tau_{2,}\sigma_2)}\beta_2(T_2 - T_a) \quad (2)$$

where D is the average Young's modulus of elasticity, $\theta_t$is the thermal expansion factor. $\Omega = D\varepsilon_0$ where $\varepsilon_0$is the initial strain and ξ is the phase transformation fraction. T is the temperature, the indices 1, 2 represent for SMA_1 and SMA_2. $\beta = \frac{h_c A_c}{m c_p}$ where h_c is heat convection coefficient,A_c is circumferential area of SMA, m is SMA mass per unit length, c_p is specific heat.

In antagonistic configuration, strain ($\varepsilon_1$andε_2) produced by SMA 1 and 2 are related as

$$\varepsilon_1 = -\varepsilon_2 \tag{3}$$

The resultant torque τ applied by the SMA wires is given by

$$\tau = (f_1 - f_2)r = (\sigma_1 - \sigma_2)Ar \tag{4}$$

where f_1 and f_2 are the forces generated by SMA_1 and SMA_2 respectively, A is the cross sectional area of the SMA wires and r is the radius of the pulley to which the actuator wires are connected. The radius of the pulley and the length of the SMA wire decide the angle of rotation and strain and torque acting on the disc respectively. From design aspect a relation is established between the angle of deflection (θ) of the beam to the strain of the SMA wire from Fig. 2.

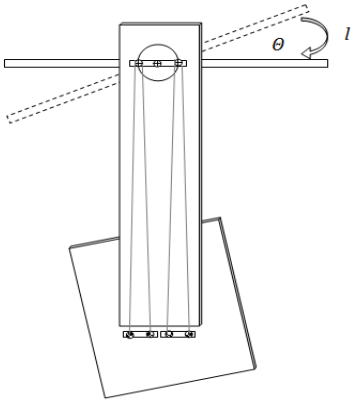

Fig. 2 Antagonistic actuation

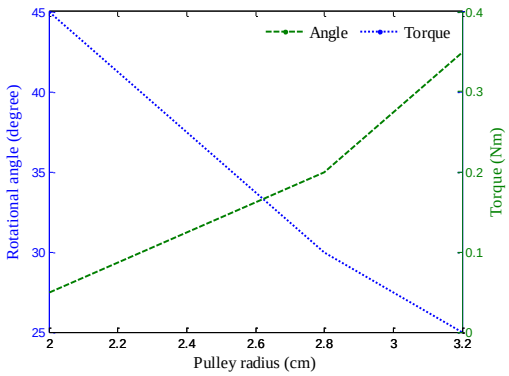

Fig. 3 Torque and angle in relation with pulley radius

The radius of the pulley and the length of the SMA wire decide the angle of rotation and strain respectively. For 4% strain of the SMA wire (according to the manufacturer's data), it offers a strain of 1.6 cm for the length of 40 cm of the wire used in the arrangement.

A relation is established between the angle of deflection (θ) of the centrally hinged one-joint arm to the arc length produced by the SMA wire.

$$\frac{2\Pi r\theta}{360^\circ} = l \tag{5}$$

$$\tau = (\sigma_1 - \sigma_2)A\frac{\varepsilon}{2\sin\frac{\theta}{2}} \tag{6}$$

$$\tau = (\sigma_1 - \sigma_2)A\frac{l}{\theta} \tag{7}$$

where l is the length of the arc which is related to the strain of the wire by $l = \frac{\varepsilon\theta}{2\sin\frac{\theta}{2}}$. Hence for any application, the angle of rotation depends on the length of the SMA actuators and the radius of the pulley. The system is designed based on the above relations. For different radius (2 cm, 4 cm, 6 cm) the variation in the angular displacement and the torque produced are shown in Fig. 3. Lesser the radius (2 cm) it produces more angles and creates lesser torque for the beam to track. Higher the pulley radius (6 cm) creates lesser angular displacement and creates higher torque. The optimum radius for this beam system is found to be 4 cm pulley radius. Hence for any application, the angle of rotation depends on the length of the SMA actuators and the radius of the pulley.

3. Modelling of the system

The ball and beam is a multi-loop system. Since the system comprises of the ball and beam mechanism and the actuator mechanism, their models are to be obtained.

Table 2 SMA specifications

SMA specifications	Value
Diameter (cm)	0.015
Length (cm)	90
Transition Temperature (^{o}C)	90
Young's modulus –Martensite (GPa)	28
Young's modulus – Austenite (GPa)	75
Approximate current at room temperature (A)	0.410
Maximum pull force (kg)	0.321

3.1 Ball and beam system

The complete description of the ball rolling on the beam is quite complicated. For control system design a simplified derivation is used to give a model that is good for controller design. The model shown in Fig. 4 shows the main components involved in the system which includes moments and forces acting on them.

Starting with the ball along the beam, it experiences a force due to the rolling constraint along the beam and a downward component due to gravity that depends on the angle of the beamθ, shown in Fig. 5

The sum of forces acting on the ball is given by Newton's second law of motion

$$\Sigma F_b = \ F_g - F_r \ = m\ddot{x} \tag{8}$$

$$F_g = mgsin\theta \tag{9}$$

$$\Sigma F_b = \ mgsin\theta - F_r \ = m\ddot{x} \tag{10}$$

where

F_b- Force acting on the ball

F_g- Force due to gravity

m- Mass of the ball

g- Acceleration due to gravity

F_r- Rolling force on the ball due to a beam angle

x - Position of the ball along the beam

By geometry the position can be defined as

$$x = \ \alpha.R \tag{11}$$

α - Angular displacement of the ball

R- Distance between the axis of the ball and point of contact of the ball with the beam, also the radius of the ball.

The torque produced by the ball's rotational motion is equal to the radius of the ball multiplied by the rotational force. Using Newton's second law of motion, the torque is equal to the ball's moment of inertia multiplied by its angular acceleration, which then can be written as its moment of inertia multiplied by the double-derivative of its translational motion (x) divided by its radius. The torque balance of the ball τ_b, is given by Eq. (12)

$$\sum \tau_b = F_r R = \ J_b \ddot{\alpha} = \ J_b \frac{\ddot{x}}{R} \tag{12}$$

$$J_b = \ \frac{2}{5} m R^2 \tag{13}$$

where

J_b-Moment of inertia of the ball

R-Radius of the ball

From above Eq. (14) the rolling force is given by

$$F_r = \ \frac{2}{5} m\ddot{x} \tag{14}$$

Substituting the above Eq. (12) gives

$$\ddot{x} = \frac{5}{7} g sin\theta \tag{15}$$

Linearising the above equation for small angle of θ and taking Laplace transform, the model of ball and beam is obtained as

$$\frac{X(s)}{\theta(s)} = \frac{5g}{7s^2} \tag{16}$$

Openloop response for the ball and beam

Open loop step response of the ball and beam model is simulated using MATLAB and the response is shown in Fig. 6. It is clearly seen that the system is unstable. Hence feedback is essential to make the system stable; also the actuator should be fast enough to reduce the acceleration of the ball thereby to stabilize the system.

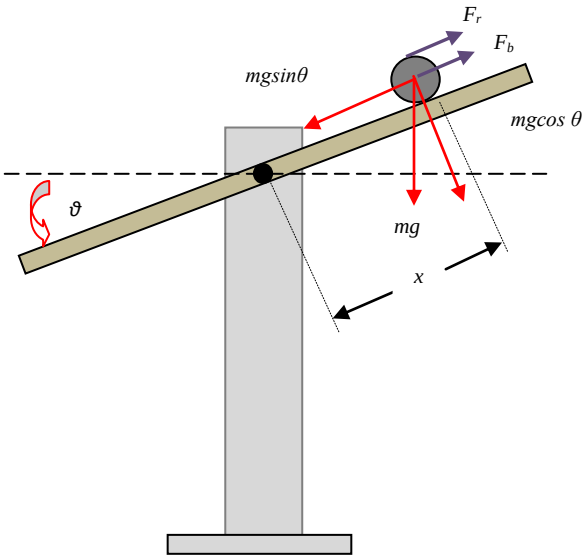

Fig. 4 Ball and beam system

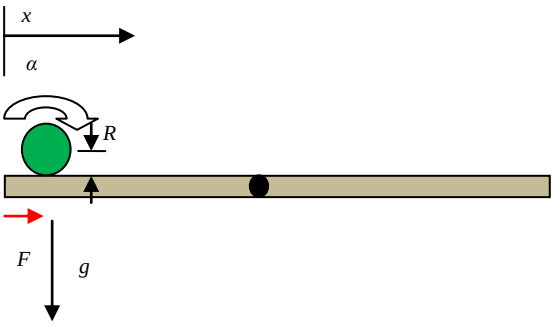

Fig. 5 Free Body Diagram of rolling ball

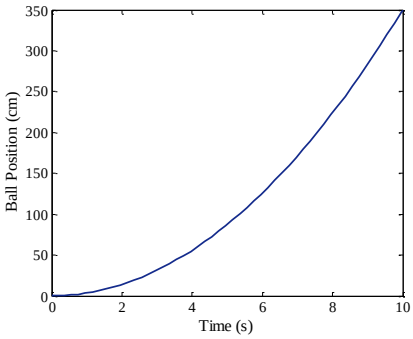

Fig. 6 Open loop response of ball and beam (simulation)

3.2 Modelling of SMA

Thermo mechanical modelling of SMA is described in literatures (Tanaka 1986, Brinson 1993, Liang 1990). But the present system requires dynamic model over a frequency bandwidth. Hence in order to obtain the model system identification method is used. System identification based on experimental approaches faithfully represents the dynamic characteristics of the system incorporated with smart materials, and avoid the tangled mathematics or physical models (Zulfatman and Rahmat 2009). It deals with the problem of building mathematical models of dynamical systems based on observed data from the system. Identification of parametric model involves selection of model structure, a numerical method for computing a model estimate and model validation. In practice, significant idea about the required plant dynamics and type of structure will assist in selecting the model structure. The prediction error estimate method based on process is selected for system identification as its estimation accuracy is good comparable with other similar methods. The sample input and output signals are as shown in Fig. 7. Dynamic input signal with frequency range of 0.1 to 2 Hz is given to the actuator and angle of the beam is measured as output. Total number of around 2305 data is collected and used for identification. In order to estimate the system model, the data is divided into two parts; the first part to determine the model and the second part is applied to validate the model. Fig. 8.depicts the validation curves for the estimated model. The estimated actuator model is

$$G(s) = \frac{4.6051}{1+0.732s} e^{-0.01s} \tag{17}$$

Here the loss function = 0.0133578 and final prediction error (FPE) = 0.0133861. The fit percentage is found to be 90.4%. Increasing the order does not improve the fit percentage, so the lowest order model with best fit is selected.

The transient response for unit step input and the frequency response are obtained through simulation and shown in Figs. 9 and 10 respectively. The bandwidth of the antagonistic SMA which cycles under complete transformation between austenite and martensite is about 1.369 rad/s and the rise time of the system is 1.61s. The bandwidth is highly influenced by the transformation strain %; under partial transformation SMA operates significantly faster than under complete transformation. During the course of control of the ball, the beam is operated within very small angular displacement and hence the SMA will be operating under partial transformation resulting in faster response. The reason behind higher speed of response is due to influence of stress acting on the antagonistic wires during operation.

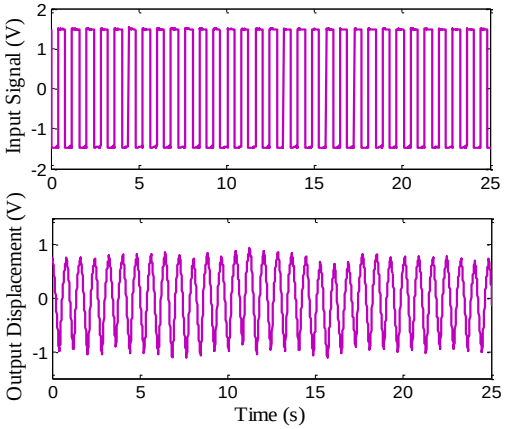

Fig. 7 Input and output signals

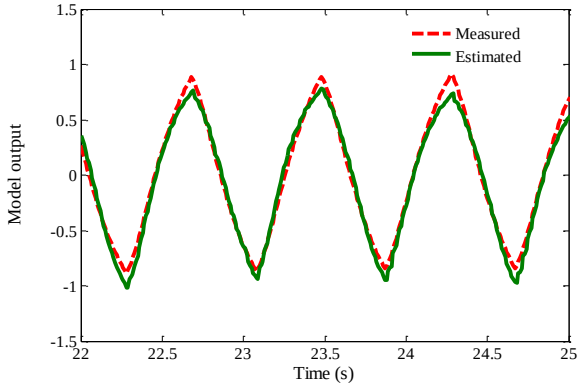

Fig. 8 Measured and predicted model output

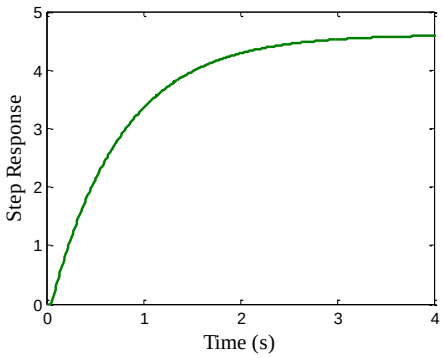

Fig. 9 Transient response of the actuator (simulation)

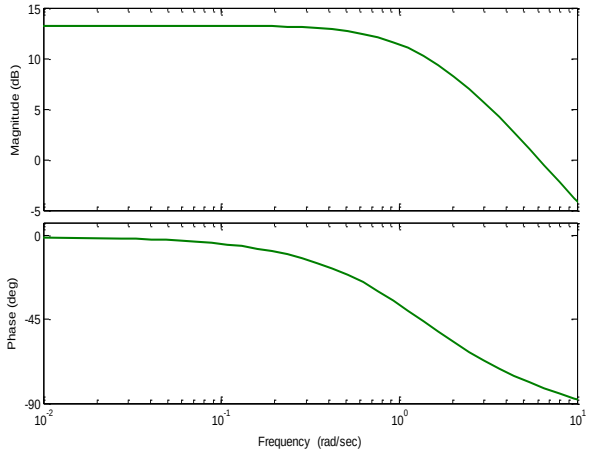

Fig. 10 Frequency response of the actuator (simulation)

4. Design of controller and experimental implementation

Fig. 11 shows the block diagram of the whole control system; it consists of two loops: (1) Inner SMA control loop (2) outer ball and beam loop. The design strategy is to first stabilize the inner loop followed by the outer loop control.

In this study settling time is considered as the control parameter, since SMA is a thermally actuated system and considered to have slow response. It is essential to study the dynamic performance of the actuator to control and stabilize within the required time. The standard time domain specification considered in conventional ball and beam system (Quanser work book 2011) for study of controller performance in laboratory is given below in Table 3.

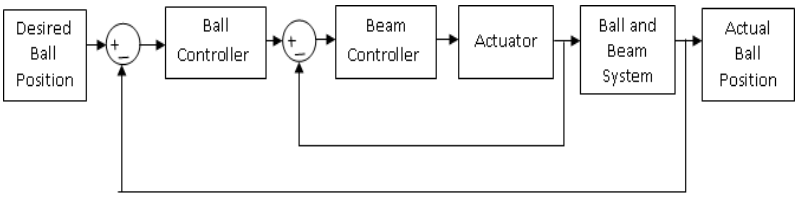

Fig. 11 Cascade control schematic of ball and beam system

Table 3 Time domain specifications

Time domain specifications	Value
Settling time(s)	< 3.5
Steady state error (cm)	0

4.1 Controller design for ball and beam

The ball and beam model is a double integrating process. In order to stabilize the ball position a PD controller is essential (Wen 2009). A mathematical description of the PD control is

$$G_{PD}(s) = K_p\left(e(t) + T_d\frac{de(t)}{dt}\right) \tag{18}$$

The proportional and derivative gains are designed based on tuning rules given in (Skogestad 2009). Here the closed loop response time τ_c is the only tuning parameter. In this case value τ_c =3s is selected such that it satisfies the time domain specifications for position control of the ball, which is most commonly used for controller design in conventional ball and beam system. The proportional and derivative gain for double integration process as shown in Eq. (5) are given by

$$G_b(s) = K\frac{e^{-\phi s}}{s^2} \tag{19}$$

$$K_p = \frac{1}{K*4(\tau_c+\phi)^2} \tag{20}$$

$$T_d = 4(\tau_c + \phi) \tag{21}$$

By using above method the controller gains are designed ($K_p = 0.003$ and$K_d = 0.2$) and optimally fine-tuned to obtain the desired specification.

4.2 Controller design for SMA actuator

Shape memory alloy model is determined by using system identification technique and is approximated to a first order model with delay. To control the angle of the beam a PID controller is designed based on Ziegler –Nichols tuning (Ziegler and Nichols 1942) using reaction curve. Mathematical description of the PID controller is given as

$$G_{PID}(s) = K_c\left(e(t) + \frac{1}{T_I}\int_0^t e(t)\,dt + T_d\frac{de(t)}{dt}\right) \tag{22}$$

As discussed above proportional, integral and derivative gain are designed ($K_p = 19.428$, $K_I = 0.0369$ and $K_d = 0.00923$).

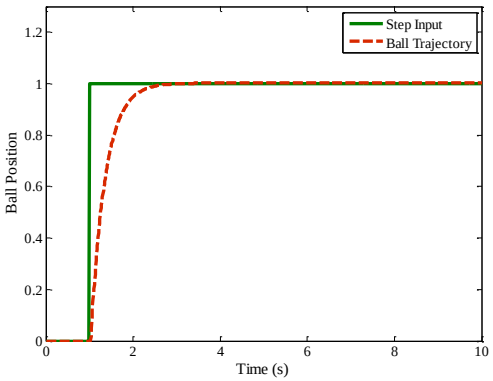

Fig. 12 Step response for the system with control (simulation)

4.3 Simulation results

The performance of the controller for the system is studied for a step input. Fig. 12 shows the simulation results which show accurate control and satisfies the time domain specification of settling time less than 3.5s.

4.4 Experimental results

Fig. 13 shows the schematic structure of the real time experimentation. Sensor signals of ball position and beam position are fedback to the PC running MATLAB and the control signal from the controller is given to the amplifier circuit via a DAQ. The objective of the system is to place the ball at desired position of the beam with control. For the desired position and actual positions of the ball as shown in Fig. 14, the control action is shown in Figs. 15 - 17 shows the ball trajectory for two other selected target position on the beam.

The PID controller is experimented for various set points along the length of the beam and the performance of the actuator is studied. It is observed from the results that SMA was able to successfully stabilize the system and the settling time of the system is well within the specifications. Considering the inherent nonlinearity of SMA and the ball and beam system itself the designed PID controller achieves stable operation. Table 4 clearly shows the nonlinearity of the system for increasing ball's acceleration as target position lies away from ball position.

When the distance between the stationary position and target position increases, the angle made by the beam also increases in order to move the ball faster and exceeds $\pm 15^{o}$, the angle assumed for linearization. Hence there is substantial change in the dynamics of the system in comparison of the model designed. This effect clearly affects the performance of the controller, Table 4 shows the performance of the controller with respect to target position and stationary position, it clearly shows as the target position distance increases from current position of the ball, the performance of the controller is getting affected. The steady state error of 2.1 cm is obtained for target position which is the outlying position from stationary position.

The main intention of this work is to study the performance of SMA for position control of complicated dynamic system. This study clearly shows the potential of antagonistically connected SMA and its ability to be used for servo control application. PID was able to stabilize the system and successfully satisfies the parameter of interest. One deficiency of the controller is presence of overshoot. Selection of much better controller is the challenge ahead in order to bring SMA's performance in phase with that of conventional motor and is taken up as the next immediate task.

Table 4 Time domain specifications

Target position from stationary position of the ball	Settling time (s)	Steady state error (cm)
Nearer	1.8	0.2
Centre	2.9	1.1
Farer	3.4	2.1

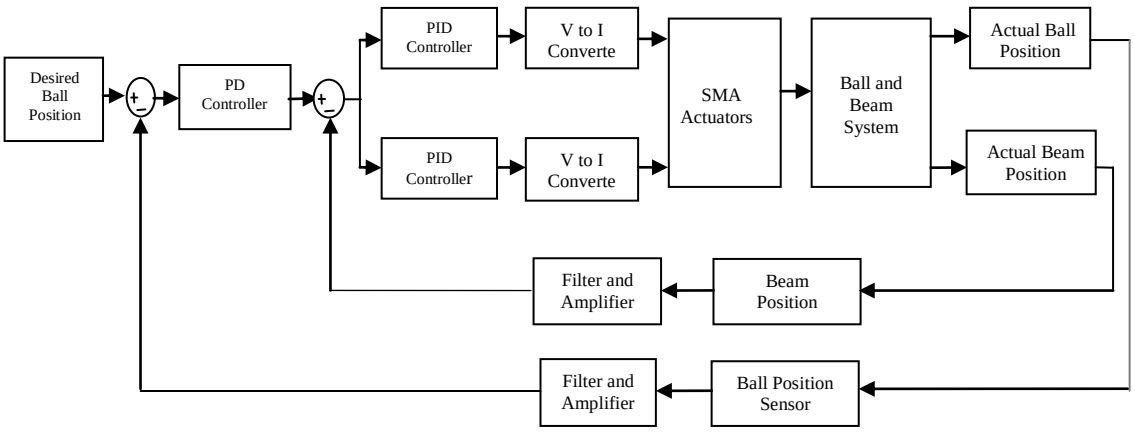

Fig. 13 Experimental implementation: Control Schematic

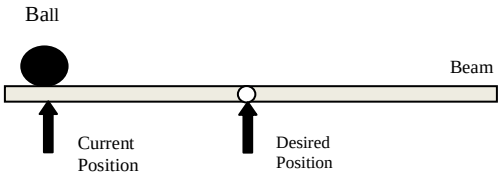

Fig. 14 Position control at centre of the beam

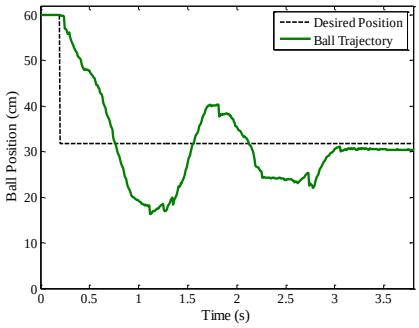

(a)

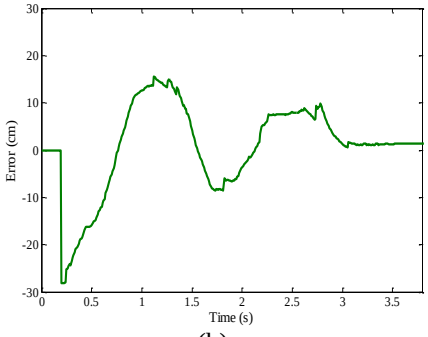

(b)

Continued-

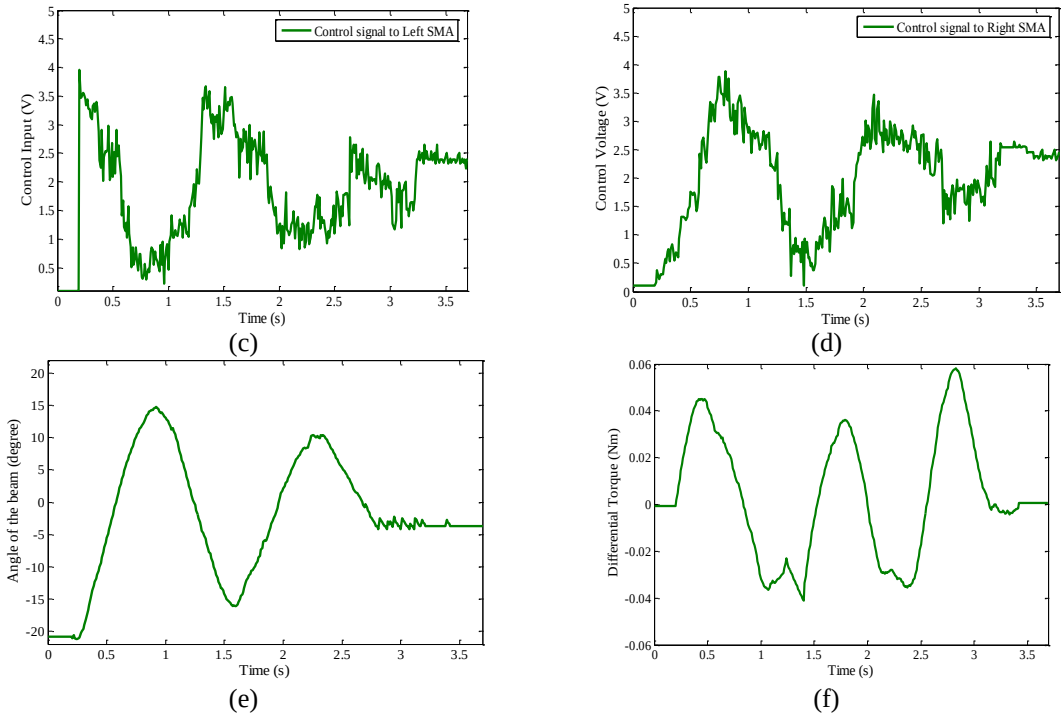

Fig. 15 (a) Trajectory of the ball, (b) Error for the ball position, (c) Control signal to left SMA, (d) Control signal to right SMA, (e) Angle of the beam and (f) Differential Torque

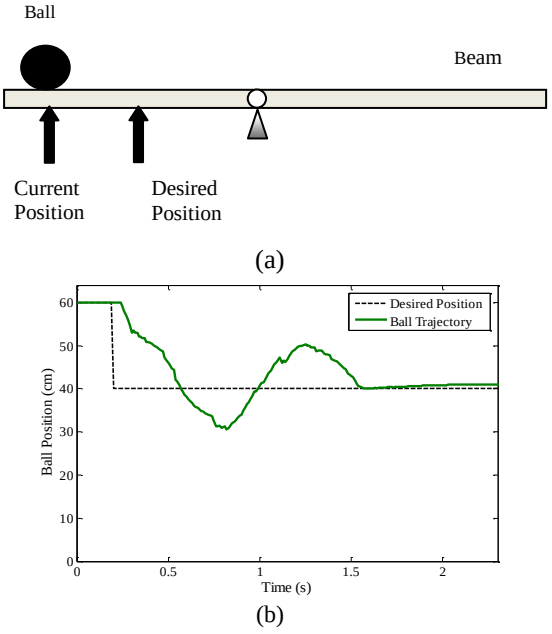

Fig. 16 (a) Target Position (near) and (b) Trajectory of the ball

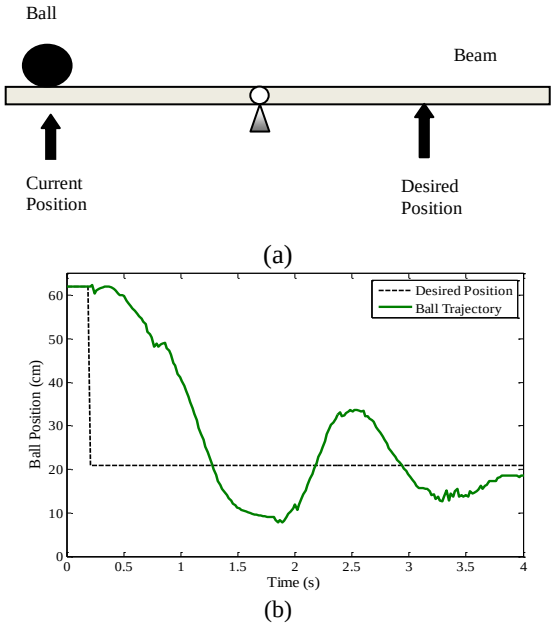

Fig. 17 (a) Target Position (far) and (b) Trajectory of the ball

5. Conclusions

The ball and beam system which is an under actuated and open loop unstable system, actuated by shape memory alloy is designed, modelled and controlled. Settling time is the parameter considered in this work to measure the performance of the actuator. This study was an attempt to understand the performance of SMA for highly dynamical system; experimental results successfully demonstrate the ability of this smart material for motion control and dynamic stabilization.SMA will offer uncompressible advantages sinceultra-light weight reducing overall weight of the system, very high force to weight ratio, literally no space and the SMA is direct driven actuator without use of any gear mechanism unlike with the use of conventional actuator in a conventional ball and beam system. In this system the weight of SMA used is 1.760 g that has controlled and stabilized the beam and ball which accounts for nearly 200 g, simultaneously handling the moments and force generated during the course of control. And also its high electrical resistivity offers self-sensing ability that would remove the need for additional sensors. Hence SMA shows a promising technology that would be a direct replacement of servo motor for critical application like aerospace and robotics.

References

Ahn, M.S. (2012), "Morphing Wing Mechanism using an SMA wire Actuator". *Int. J. Aeronaut. Space Sci.*, **13**(1), 58-63.

Brinson, L.C. (1993), "One dimensional Constitutive behaviour of shape memory alloys: Thermo mechanical derivation with non-constant material functions and redefined martensite internal variable", *J.*

Intel. Mat. Syst. Str., **4**(2), 229-242.
Dhanalakshmi, K., Umapathy, M., Ezhilarasai, D. and Bandyopadhyay, B. (2011), "Design and implementation of fast output sampling feedback control for shape memory alloy actuated structures", *Smart Struct. Syst*., **8**(4), 367-384.
Donmez, B. and Ozkan, B. (2011), "Design and control of a shape memory alloy actuator for flap type aerodynamic surfaces", *Proceedings of the IFAC World Congress*, Italy, August.
Feng, Y., Rabbath, C.A., Hong, H., Janaideh, M.A. and Su, Y.C. (2010), "Robust Control for Shape Memory Alloy Micro Actuators Based Flap Positioning System", *Proceedings of the IEEE American Control Conference*, Baltimore, June.
Georges, T., Brailovski, V., Morellon, E., Coutu, D. and Terriault, P. (2009), "Design of shape memory alloy actuators for morphing laminar wing with flexible extrados", *J. Mech. Design*, **131**(9), 091006.
Liang, C. and Rogers, C.A. (1990), "One-dimensional thermo mechanical constitutive relations for shape memory materials", *J. Intel. Mat. Syst. Str*., **1**(2), 207-234.
Moallem, M. and Tabrizi, V.A. (2008), "Tracking control of an antagonistic shape memory alloy actuator pair", *IEEE T. Contr. Syst. T.*, **17**(10), 184-190.
Mohammad, H.E., Seigler, M., Leo, J.D. and Ahmadian, M. (2006), "Nonlinear stress-based control of a rotary SMA actuated manipulator", *J. Intel. Mater. Syst. Str*., **15**(6), 495-508.
Quanser Ball and beam workbook student version (2011)
Ruth, D.J.S., Nakshatharan, S.S. and Dhanalakshmi, K. (2012), "Angular trajectory tracking using antagonistic shape memory alloy actuators", *Proceedings of the IEEE International Conference on Sensing Technology*, India.
Ruth, D.J.S., Nakshatharan, S. S. and Dhanalakshmi, K. (2013),"Auto-adaptive control of a one-joint arm direct driven by antagonistic shape memory alloy", *Int. J. Smart Sens. Intell. Syst.*, **6**(3), 833-849.
Sars. V.D., Haliyo, S. and Szewczyk. J. (2010), "A practical approach to the design and control of active endoscopes", *Mechatronics*, **20**(10), 251-264.
Singh, P. and Ananthasuresh, G.K.A. (2013), "Compact and compliant external pipe – crawling robot", *IEEE T. Robot*, **29**(1), 251-260.
Song, G., Ma, N., Li, L., Penney, N., Barr, T., Lee, H.J. and Arnold, S. (2011),"Design and control of a proof-of-concept active jet engine intake using shape memory alloy actuators", *Smart Struct. Syst*., 7(1), 1-30.
Skogestad, S. (2009), "Simple analytic rules for model reduction and PID controller tuning", *J. Process Contr.*, **13**, 291-309.
Tanaka, K. (1986), "A thermo mechanical sketch of shape memory effect: One dimensional tensile behaviour", *Res. Mech*., **18**, 251-263.
Tharayil, M.L. and Alleyne, G.A.(2004), "Modeling and control for smart-meso flap aero elastic control", *IEEE – ASME T. Mech.*, **9**(1),141-149.
Wen, Y. (2009), "Nonlinear PD regulation for ball and beam system", *Int. J. Elec. Eng. Educ.*, **46**(1), 59-73.
Williams, E.R., Shaw, G. and Elahinia, M. (2010), "Control of an automotive shape memory alloy mirror actuator", *Mechatronics*, **20**(5), 527-534.
Youssef, M.A. and Elfeki. M.A. (2012). "Seismic performance of concrete frames reinforced with super elastic shape memory alloys", *Smart Struct. Syst*., **9**(4), 565-585.
Ziegler, J.G. and Nichols, N.B. (1942), "Optimum settings for automatic controllers", *Trans. ASME*, **64**, 759-768.
Zulfatman, Z. and Rahmat, M.F. (2009), "Application of self-tuning fuzzy PID controller on industrial hydraulic actuator using system identification approach", *Int. J. Smart Sensing Intell. Syst.*, **2**(2), 246-261.